Multi-level discrete fracture model for carbonate reservoirs

Li, L.; Voskov, D.

DOI
10.3997/2214-4609.201802164

Publication date
2018

Document Version
Final published version

Published in
16th European Conference on the Mathematics of Oil Recovery, ECMOR 2018

P034

Multi-Level Discrete Fracture Model For Carbonate Reservoirs

L. Li (Research Centre of Multiphase Flow in Porous Media, China University of Petroleum (East China)), D. Voskov* (Civil Engineering & Geosciences, Delft University of Technology)

Summary

The main challenge for predictive simulation of carbonate reservoirs is associated with large uncertainties in the geological characterization with multiple features including fractures and cavities. This type of reservoirs requires robust and efficient forward-simulation capabilities to apply data assimilation or optimization technique under uncertainties. The interaction between reservoir matrix and various features introduces a complex multi-scale flow response driven by global boundary conditions. The Discrete Fracture Models (DFM), which represent fractures explicitly, is capable to accurately depict all important features of flow behavior. However, these models are constrained by many degrees of freedom when the fracture network becomes complicated. The Embedded DFM, which represents the interaction between matrix and fractures analytically, is an efficient approximation. However, it cannot accurately reproduce the effect of local flow conditions, especially when the secondary fractures are present. In this study, we applied a numerical upscaling of DFM a triple continuum model where large features are represented explicitly using the numerical EDFM and small features are upscaled as a third continuum. In this approach, we discretize the original geo-model with unstructured grid based on DFM and associate the mesh geometry with large features in the model. Using the global solution, we generate local boundary conditions for the model capturing the response of primary features to the flow. Applying local boundary conditions, we resolve all secondary features using a fine scale solution and update the local boundary conditions. This procedure is applied iteratively using the local-global-upscaling formalism. To demonstrate the accuracy of the Multi-Level Discrete Fracture Model, several realistic cases have been tested. By comparing with fine scale DFM solution and the traditional EDFM technique, we demonstrate that the proposed model is accurate enough to capture the flow behavior in complex fractured systems with advanced computational efficiency.

Introduction

With the development of exploration techniques and theories, more carbonate reservoirs have been discovered and utilized recently. As referred in Schlumberger Market Analysis (2007), more than 60% of the world's oil and 40% of the world's gas reserves are held in carbonates. However, it is always a big challenge to predict the production from carbonate reservoirs due to the large uncertainties in characterization with multiple features including fractures and cavities. The accurate prediction of production dynamics requires uncertainty quantification and data assimilation procedures to determine reasonable development plan. For that, robust and efficient forward simulation capabilities are strongly required.

There are many models which have been proposed for the carbonate reservoir simulation. The first attempt to represent the fluid flow in fractured porous media had been made by Barrenblatt *et al*. (1960) which was later extended by Warren and Root (1963) to the dual-porosity (DP) models into petroleum reservoir engineering. Next, the dual-porosity dual-permeability (DPDK) model has been introduced (Gerke *et al*., 1993a; Gerke *et al*., 1993b). Currently, the DP and DPDK models are widely used in the commercial reservoir simulators (Eclipse, 2009; CMG, 2013). Being constrained by an implicit representation of fractures, these models are limited to predict the flow response in carbonate systems accurately enough.

To improve the representation of flow in fracture reservoirs, Pruess and Narasimhan (1982, 1985) developed a multiple interacting continuum model (MINC) which can be seen as an extension of DP concept. Different from the DP and DPDK models, MINC model can represent more accurately transient effects within the porous matrix. Constrained by assumptions originated from DP concept, it can only be used in situations when fractures are well connected. To make the fractured reservoir simulation flexible for structured grids and represent the fractures explicitly, an embedded discrete fracture model (EDFM) has been developed by Lee *et al*. (2000) and Li and Lee (2008). In EDFM, non-conforming grids are applied for the fracture-matrix connections. To extend the application of EDFM, Tene *et al*. (2017) later proposed a project-embedded discrete fracture model (pEDFM) where fracture networks have a wide range of conductivities.

To capture the fine-scale flow response accurately, Karimi-Fard *et al*. (2004) developed a discrete fracture and matrix (DFM) model which reduces the dimensionality of the fracture representation in the mesh. Due to the explicit representation of fractures, DFM is by far the most accurate approach for modelling of fractured reservoirs. However, the DFM application can lead to a large number of control volumes which in turn reduces the computational efficiency. To overcome the drawbacks of DFM, several upscaling approaches were proposed (Karimi-Fard *et al*., 2006; Gong, 2007; Karimi-Fard *et al*., 2012; Karimi-Fard *et al*., 2016). In addition, the DFM approach was extended to account for geomechanics effects (Garipov *et al*., 2016) and fracture propagation (Gallyamov *et al*., 2018).

In this study, we propose a multi-level discrete fracture model (MLDFM), which takes full advantage of the accuracy of DFM and the flexibility of EDFM and is capable to capture the multi-scale flow response related to complex carbonate reservoirs. In this approach, we apply a numerical upscaling of fine-scale DFM characterization to a triple continuum model where large features are represented explicitly using the numerical EDFM and small features are upscaled as third continuum. We construct two levels of grids: the coarser structured grids are used for forward-simulation and capture the main flow response; the finer unstructured grids, which represent small features explicitly, are used for resolving fine-scale flow response and computing the connectivity with numerical upscaling technique. To integrate the multi-scale flow response, the main flow response from a coarse-scale model is applied to generate local boundary conditions for a fine-scale simulation. In this approach, the effect of local flow conditions on the multi-scale flow response can be considered. However, the local flow conditions driven by global boundary conditions are not static. To update the dynamic local flow conditions according to global boundary conditions, we apply the local-global formalism based on which the interactions between different features can be updated once the local flow conditions have been

changed. The MLDFM approach is illustrated by several test-cases to demonstrate its robustness, accuracy and efficiency.

Modeling approach

The model is numerically solved using the Automatic Differentiation General Purpose Research Simulator (ADGPRS) (Voskov, 2012; Zaydullin *et al*., 2014; Garipov *et al*., 2016, 2018).

Conservation equations

In this study, the dead-oil model is applied. The mass conservations of oil and water phases can be written as follows:

$$\frac{\partial}{\partial t}\left(\phi\rho_o S_o\right)+\nabla\cdot\left(\rho_o\mathbf{u}_o\right)+\rho_o q_o=0, \tag{1}$$

$$\frac{\partial}{\partial t}\left(\phi\rho_w S_w\right)+\nabla\cdot\left(\rho_w\mathbf{u}_w\right)+\rho_w q_w=0. \tag{2}$$

where ϕ is the reservoir porosity; t is the time; subscripts o and w indicate oil and water phases; ρ is the phase molar density; S is the saturation; q is the source/sink term; $\mathbf{u}$ is the velocity:

$$\mathbf{u}_j=-\frac{kk_{rj}}{\mu_j}\nabla P \tag{3}$$

where μ is viscosity; k is the permeability; k_{rj} is the relative permeability of phase j; P is the reservoir pressure.

The saturation constraint is used to close the system:

$$S_o+S_w=1 \tag{4}$$

Apply the two-point flux approximation (TPFA) finite volume discretization and the backward Euler approximation discretization in time, the fully-implicit approximation of (1) can be written as:

$$\begin{aligned}&\Delta t\sum_l\left(\rho_o^l\lambda_o^l\gamma^l\Delta\psi^l+\rho_w^l\lambda_w^l\gamma^l\Delta\psi^l\right)^{n+1}+\Delta t\left(\rho_o q_o+\rho_w q_w\right)^{n+1}\\&-\left[V\phi\left(\rho_o S_o+\rho_w S_w\right)\right]^{n+1}+\left[V\phi\left(\rho_o S_o+\rho_w S_w\right)\right]^{n}=0\end{aligned} \tag{5}$$

Here Δt is the time step; V is the volume of grid cell; $\Delta\psi^l$ is the potential difference over interface l; $\lambda_j^l=\left(k_{rj}/\mu_j\right)^l$ is the mobility of phase j over the interface l by upstream weighting; n+1 is the current time step; n is the previous time step; γ is the transmissibility.

To represent the dynamic of flow in carbonate reservoirs accurately, the DFM model is applied in this study following Karimi-Fard *et al*. (2004). The transmissibility between matrix blocks is written as:

$$\gamma_{mimj}=\frac{\alpha_{mi}\alpha_{mj}}{\alpha_{mi}+\alpha_{mj}}\qquad\alpha_{mi}=\frac{k_m^i A_m^i\mathbf{n}_i^l\mathbf{f}_i^l}{L_m^i}, \tag{6}$$

where subscript m indicates matrix grid, subscripts i and j mean the two neighbouring grids connected by l interface; A^l is the area of the interface l; $\mathbf{n}_i^l$ is the unit normal to the interface l inside grid i; $\mathbf{f}_i^l$ is the unit vector along the direction of the line joining the volume centroid to the centroid of the interface l; L_m^i is the length of the line joining the volume centroid of grid i to the centroid of the interface l.

The transmissibility between matrix block and fracture element is defined as:

$$\gamma_{mifj}=\frac{\alpha_{mi}\alpha_{fj}}{\alpha_{mi}+\alpha_{fj}}\qquad\alpha_{mi}=\frac{k_m^i A_m^i\mathbf{n}_i^l\mathbf{f}_i^l}{L_m^i},\alpha_{fj}=\frac{k_f^j A_f^j\mathbf{n}_j^l\mathbf{f}_j^l}{L_f^j}, \tag{7}$$

where f indicates fracture element. Finally, the transmissibility between the elements of two or more fractures is given by:

$$\gamma_{fifj} = \frac{\alpha_{fi}\alpha_{fj}}{\sum_{k=1}^{n}\alpha_{fk}} \qquad \alpha_{fi} = \frac{k_f^i A_f^i}{L_f^i}. \tag{8}$$

Due to the explicit representation of fractures, which leads to a large number of control volumes for complex fractured reservoir, DFM model is usually among the most computational expensive technique for fractured reservoir simulation. While DFM discretization is largely used as high-fidelity models for fractured reservoirs due to their accuracy, various alternative models, such as DP, DPDK, MINC, EDFM and MSR, are still widely used in the industry as proxy models due to their computational efficiency.

Impact of local boundary conditions

As the complex multi-scale flow response, driven by various features, is closely related to the flow condition, we demonstrate first the effect of local boundary conditions on the interaction between matrix and fractures using a simplified geo-model shown in Figure 1.

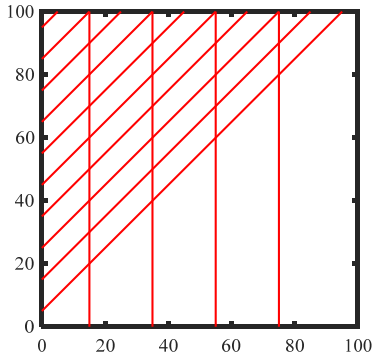

Figure 1 *A fractured network in local region.*

By injecting water at left or down boundary of the fracture network, we obtain the pressure and saturation distributions shown in Figure 2. The comparison of the solutions in Figure 2a and Figure 2b demonstrates that the local flow conditions have a large effect on the interaction between matrix and fracture network. Some fractures can be activated or inactivated with the variation of local flow conditions. Therefore, we can conclude that, the direct implicit representation of the fractures, used in DP and DPDK models, cannot reproduce the differences in the local flow response accurately enough. The existence of one fracture can affect the interaction between matrix and other fractures, and their interactions varies with local boundary conditions. Therefore, the transmissibility between different features should be updated with the local flow condition. As the traditional MINC, EDFM and MSR usually represent the interaction between matrix and fractures with fixed transmissibility, it is difficult to reproduce the complex multi-scale flow response using them.

a) *pressure and saturation distributions when water is injected from the left*

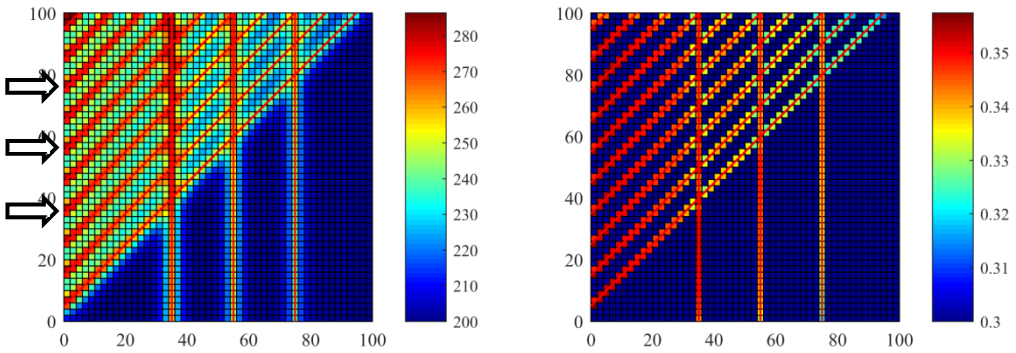

b) *pressure and saturation distributions when water is injected from the bottom*

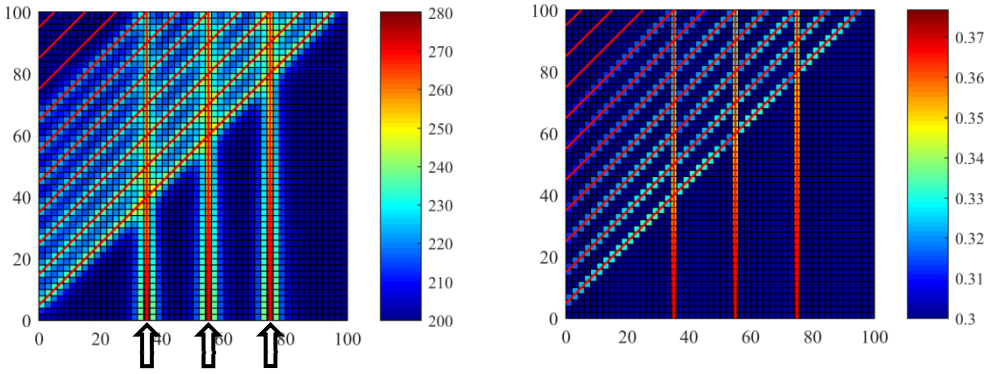

Figure 2 *The effect of local flow conditions on the flow response.*

In this study, we propose a multi-level discrete fracture model (MLDFM) where large features are represented explicitly using the numerical EDFM and small features are upscaled as a third continuum. To make sure that our model can capture the complex multi-scale flow response accurately, we apply the local-global upscaling technique which can update the transmissibility between different features according to changes in local flow conditions.

Multi-Level Discrete Fracture Model for Carbonate Reservoirs

Here, we describe the proposed method in all details using a realistic geo-model shown in Figure 3a. In this model, we have two sets of features: the large-scale fractures (in yellow) and the small-scale fractures (in blue). First, we discretize the geo-model with structured grids shown in Figure 3b. The discretized model at this stage is used for coarse-scale forward-simulation with an application of the triple continuum model. The small-scale fractures fall inside the same structured grid are upscaled as a third continuum in addition to the large-scale discrete fractures and matrix.

Second, to generate a triple continuum model, we split the whole domain into subdomains and perform local upscaling in each subdomain. The subdomains are represented as coarser structured grids shown in Figure 4a. Third, to insure a robust and accurate local upscaling, we need to extend the subdomains. With the red grids shown in Figure 4a, we can determine an extended region for each subdomain. Fourth, to perform the local upcaling in the final step, we need to determine the boundary conditions in each subdomain.

The large-scale fractures (in yellow) and purple lines obtained from red grids, shown in Figure 4b, are taken as boundaries to constrain the local flow condition. The pressure values on the boundary are determined in the following approach: the pressure of large-scale fractures are taken from coarse-scale forward simulation; the pressure values on the positions corresponding to the centroids of coarse-scale structured grids are taken from coarse-scale forward simulation; the pressure values on other positions of the boundaries can be resolved with interpolation or basis function approach used in multiscale finite volume method (Hajibeygi *et al*., 2011; Wang and Tchelepi, 2014; Tene *et al*., 2015).

Finally, we perform local upscaling for each subdomain. We pick out a subdomain shown in Figure 5a, then include all small fractures into the local region shown in Figure 5b and mesh the domain with fine unstructured grid constructed using Gmsh (Geuzaine, 2009). With the known boundary conditions, we perform a steady state simulation. Next, we can reproduce the fine-scale flow response. Based on this flow response, we compute transmissibilities between various continua: matrix and large fractures, matrix and small fractures and small fractures and large fractures. For transmissibility computation we use a numerical upscaling approach. Among the upscaling methods discussed in Durlofsky (2012), we adapt the single-phase flow-based upscaling in this study.

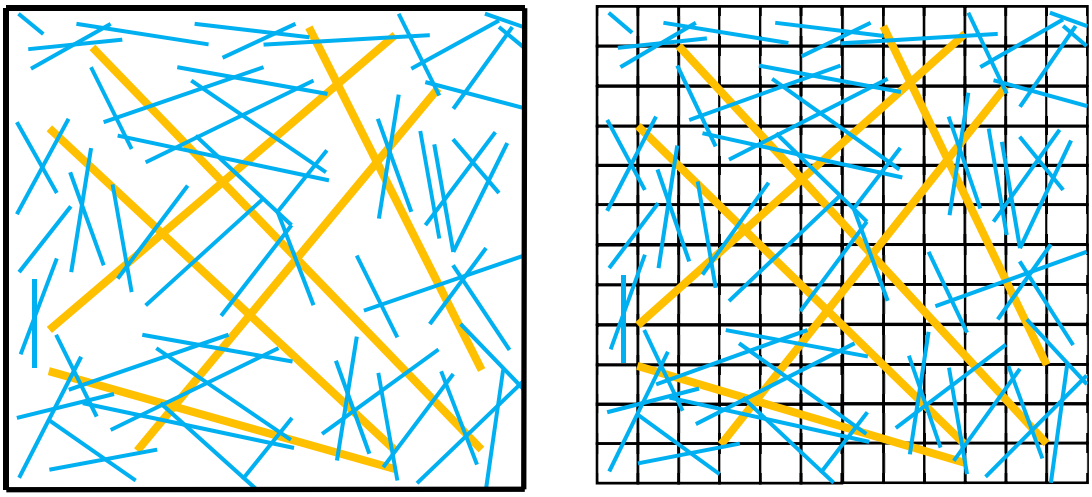

Figure 3 *The geo-model of fractured reservoir(left) and meshed structured grids(right).*

The steady-state simulation is performed on local region based on the governing equation:

$$\nabla\left[k^f \nabla p^f\right] = 0\,. \tag{9}$$

The flux through a fine-scale interface l is defined as:

$$\left(q^f\right)_l = \left(T^f \Delta p^f\right)_l\,. \tag{10}$$

The flux between coarse-scale control volumes can be written as:

$$q^c = \sum_l \left(q^f\right)_l\,. \tag{11}$$

The pressure of coarse-scale control volumes can be computed with volume-average method:

$$p_m^c = \left\langle p^f \right\rangle_m \qquad p_n^c = \left\langle p^f \right\rangle_n, \tag{12}$$

where subscripts m and n mean two connected control volumes in coarse-scale; $\langle\varphi\rangle_m$ denotes a bulk-volume-averaged property computed over the fine-scale control volumes which are inside the coarse control volume m. Then the transmissibility between coarse-scale control volumes can be written as:

$$T_{m,n}^c = \frac{\sum_l \left(q^f\right)_l}{abs\left(\left\langle p^f \right\rangle_m - \left\langle p^f \right\rangle_n\right)}\,. \tag{13}$$

Note that in the first step, the pressure distribution on coarse-scale can be obtained with a simulation based on traditional EDFM.

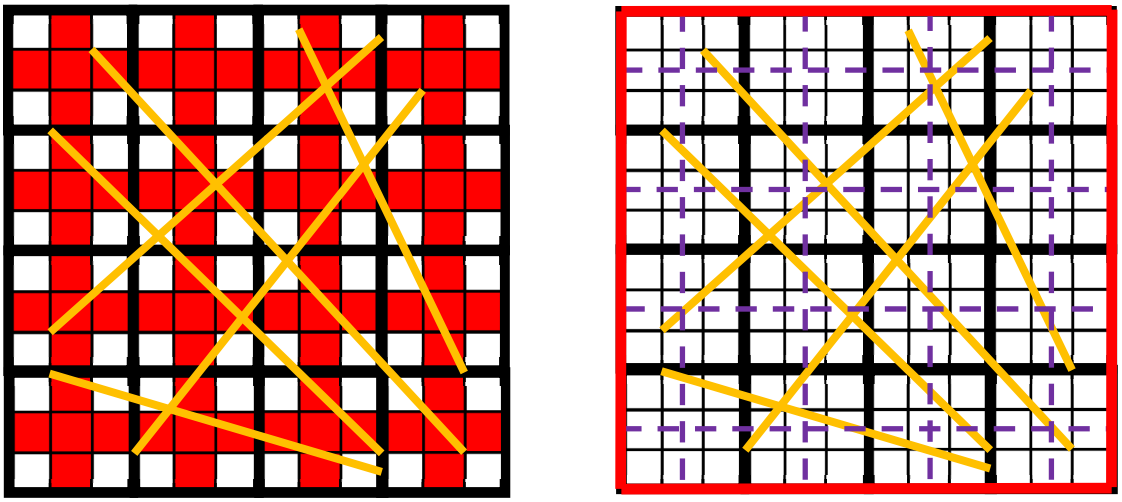

Figure 4 *Coarser structured grid (left) and boundary lines (right).*

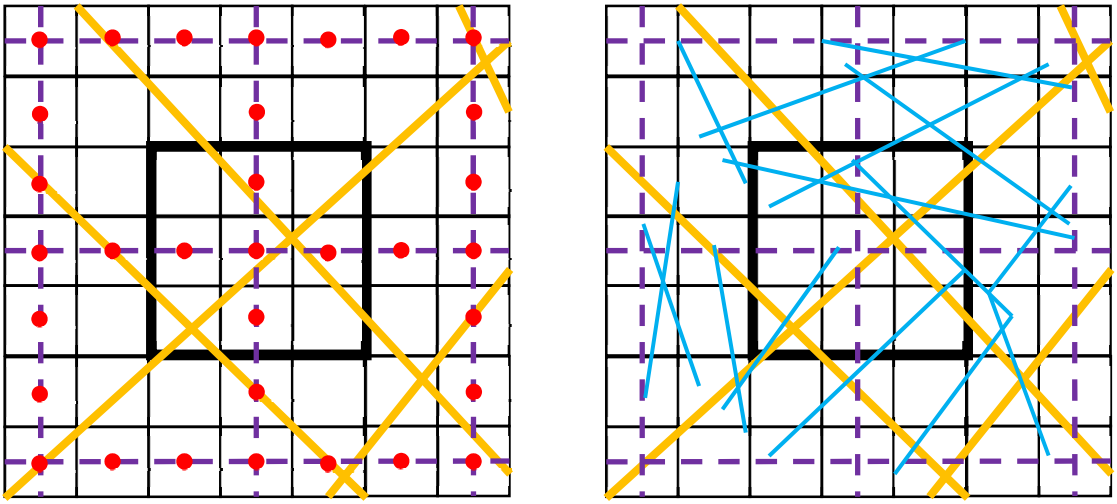

Figure 5 *The local boundary conditions for coarse features (left) and the same region with all features included (right).*

Adaptive local-global upscaling

As discussed in Renard *et al.* (1997) and Miller *et al.* (1998), the local boundary conditions are quite important in local upscaling techniques. Due to adjustments in field development strategy and the variety of multiscale heterogeneities, the local boundary conditions cannot be fixed. Therefore, dynamic local boundary conditions, which are adapted to the dynamic situation, are required to accurately reproduce the multiscale flow response in fine-scale simulation. To achieve this goal, the adaptive local-global (ALG) upscaling formalism described in Chen (2003) and Li (2014) is adopted in our study. We determine the local Dirichlet boundary conditions from coarse-scale forward-simulation solutions (the first step described above) based on interpolation or basis function approach used in multiscale finite volume method. Considering the fact that the local boundary conditions are stable during this process, we only perform the ALG upscaling once the local boundary conditions have been changed.

Numerical results

In this section, we validate the accuracy and feasibility of the Multi-Level DFM strategy to capture the multi-scale flow response in fractured systems. Next, we apply it to several examples of practical interest and study the sensitivity of the proposed method to the flow condition, and fracture orientation. We also study the feasibility of the MLDFM method for realistic fractured reservoirs.

Basic single-phase flow response

In this section, we construct a simple fracture network shown in Figure 6. Then we compare the reference high resolution DFM solution against EDFM where all fractures are represented explicitly and against MLDFM. The reference DFM solution is based on the conformal grid and numerically converged, see Satori (2018) for details. The geometry parameters and fluid properties are taken from Tables 1, 3 and 4 in Appendix A. The model studies a single-phase flow with the constant rate boundary conditions specified at 200 m^3/day on the left and right boundaries when upper and lower boundaries was set to no-flow conditions. The simulation is run for 1000 days.

The pressure distributions, obtained from simulation with DFM, EDFM and MLDFM models, are shown in Figure 7. The results demonstrate that the MLDFM model is capable to capture the main flow response caused by an idealistic fracture system and produces similar results to the DFM approach and slightly better results than the EDFM approach. Next, we compare the pressure distribution of both solutions in Figure 8. The mean square errors of the EDFM and MLDFM compared with DFM are equal to 0.638 and 0.399 respectively. It shows that the implementation of MLDFM can improve the accuracy by 37.5% compared with EDFM for a single phase flow.

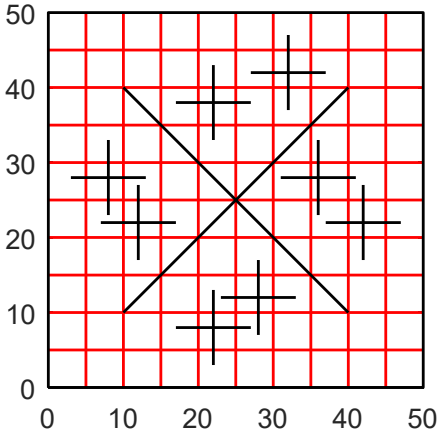

Figure 6 *The schematic of a simple fracture network.*

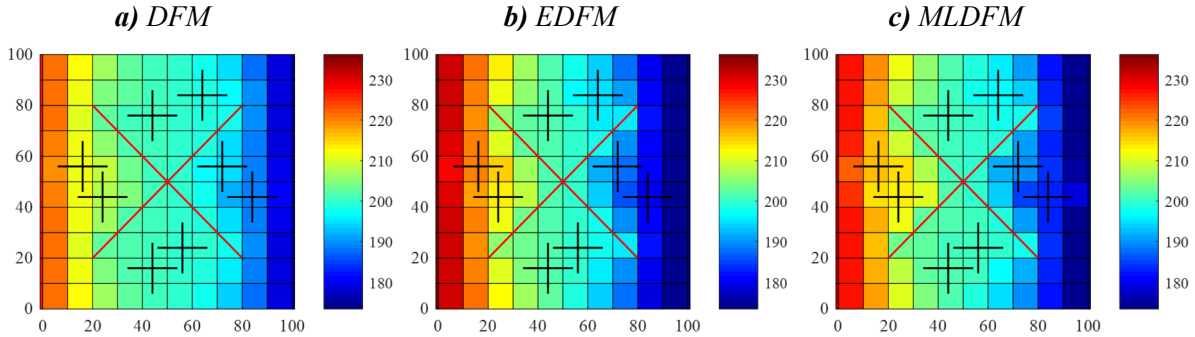

Figure 7 *The pressure distributions obtained from DFM, EDFM and MLDFM.*

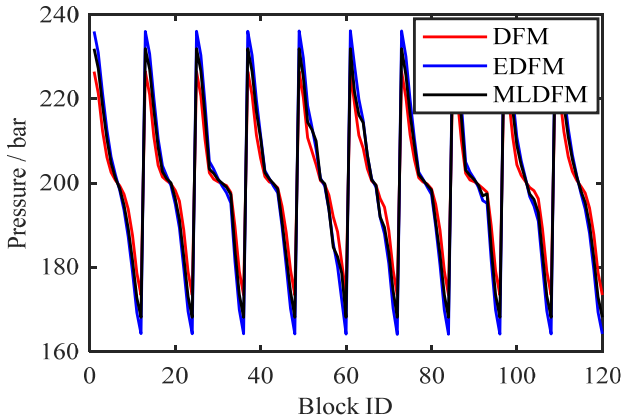

Figure 8 *The comparison of pressure solutions obtained from DFM, EDFM and MLDFM.*

Multi-phase multi-scale flow response

Next, we test the fractured model shown in Figure 9 to demonstrate the capability of MLDFM to capture the multi-scale flow response. The geometry parameters, relative permeability, fluid properties and injection/production strategy are taken from Tables 1- 5 in Appendix A.

We compare the reference high resolution DFM solution against hybrid model of EDFM with Equivalent Continuum Model (EDFM + ECM) and MLDFM. Regarding the EDFM + ECM, the large-scale fractures are represented explicitly; the small-scale fractures are taken as matrix continuum and contribute to the matrix permeability using upscaling technique. The models were compared at the same

boundary conditions as described in previous example except that the water is injected from the left side.

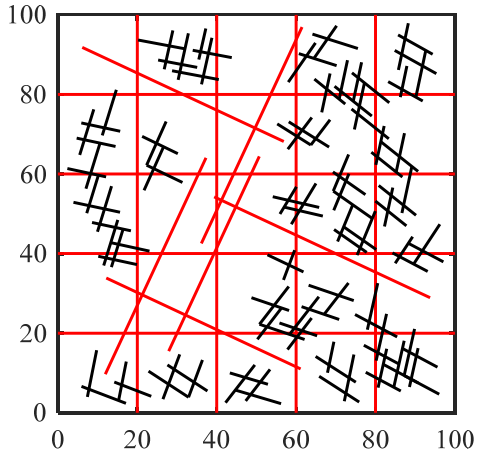

Figure 9 *The schematic of fracture network.*

As shown in Figures 10 and 11, the fracture network generates a complex multi-scale flow response. The saturation distribution shown in Figure 10 demonstrates that MLDFM is capable to predict the main flow path more accurate than EDFM + ECM. The pressure solutions shown in Figure 11 demonstrates that MLDFM improves the simulation accuracy compared with EDFM + ECM. The mean square errors of the EDFM + ECM and MLDFM compared with DFM are equal to 4.108 and 1.101 respectively. The implementation of MLDFM can improve the accuracy by 73.2% compared with EDFM + ECM in multi-phase flow.

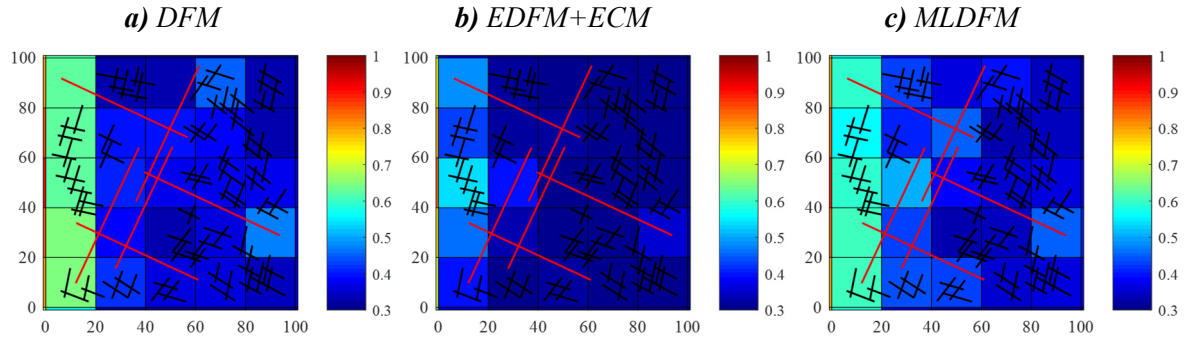

Figure 10 *The water saturation distributions.*

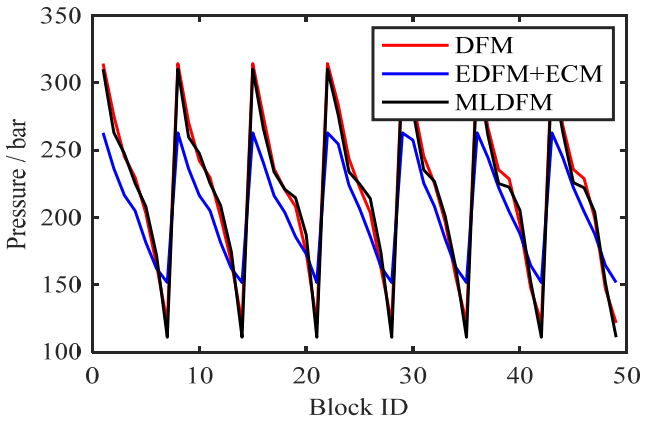

Figure 11 *The pressure distributions.*

Sensitivity to flow conditions

As discussed above, boundary conditions have a large effect on the multi-scale flow response. Here, we will test the sensitivity of MLDFM solutions to flow conditions with the fracture networks shown in Figure 9. The geometry parameters, relative permeability, fluid properties and injection/production strategy are taken again from Tables 1-5 in Appendix A. The flow directions are shown in Figure 12. As the solution for the first flow conditions is already shown in Figures 10 and 11, we only include here the second and third flow conditions. The saturation distributions, presented in Figures 13 and 14, demonstrate that MLDFM is capable to predict the main flow path more accurately than EDFM + ECM. The pressure solutions shown in Figures 15 and 16 demonstrate that MLDFM can improve the simulation accuracy quite significantly compared with EDFM + ECM at different boundary conditions. The improvement of the accuracy of MLDFM compared with EDFM + ECM for the second and third flow conditions are equal to 65.0% and 51.4% respectively. It demonstrates that MLDFM is flexible to different flow conditions and can be applied for the simulation of complex and realistic fracture networks.

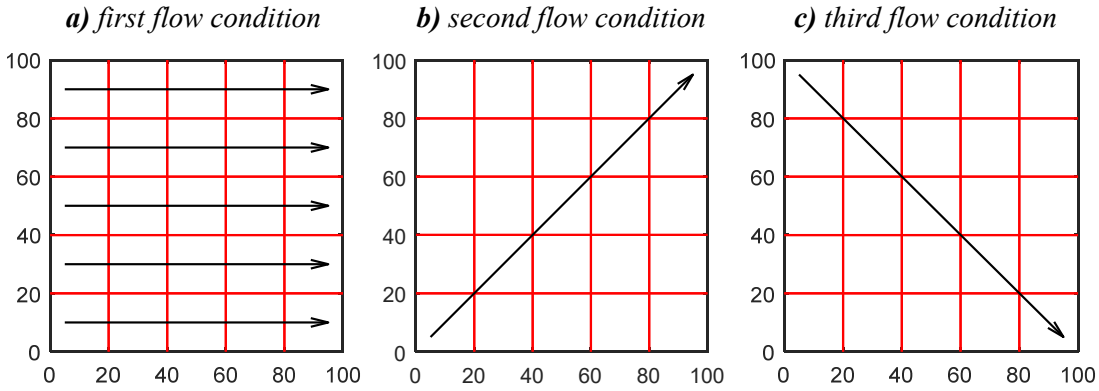

Figure 12 *The schematic of three flow conditions.*

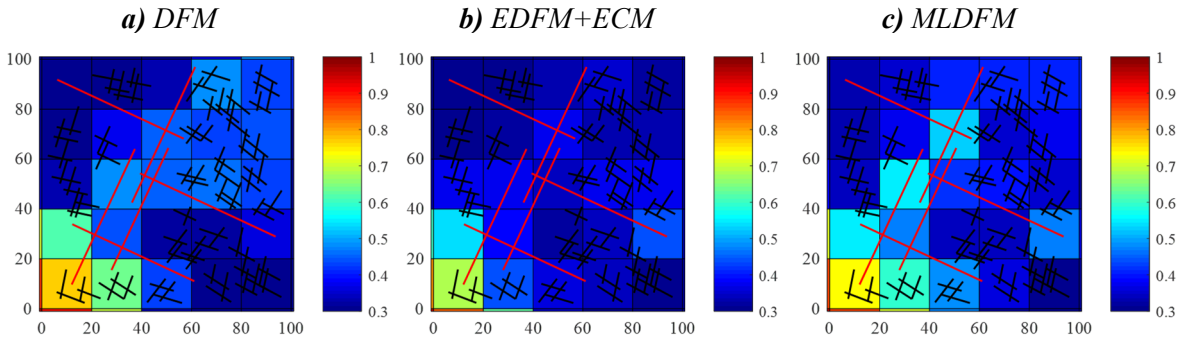

Figure 13 *The water saturation distributions at second flow condition.*

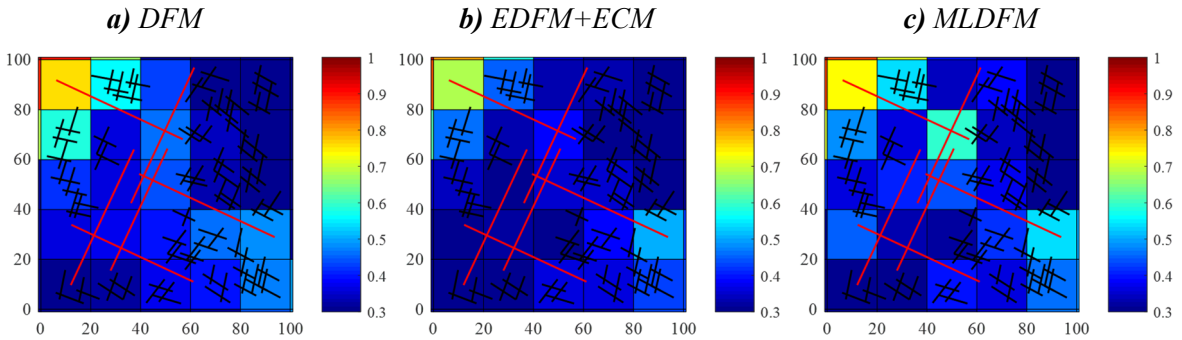

Figure 14 *The water saturation distributions at third flow condition.*

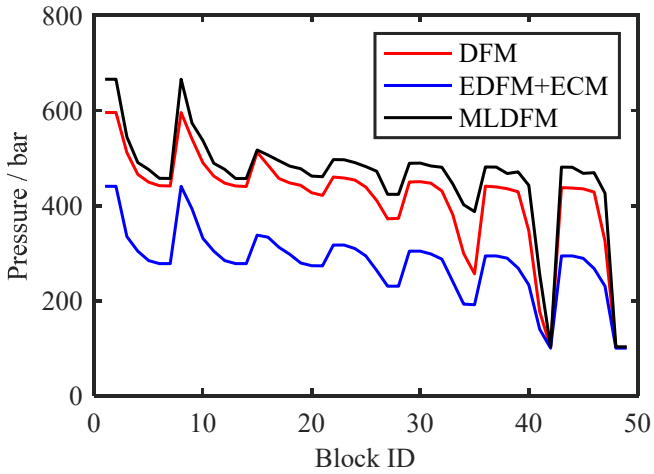

Figure 15 *The pressure distributions at second flow condition.*

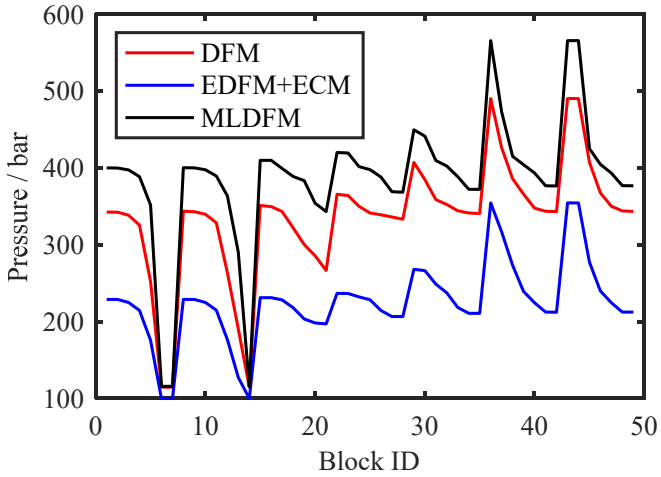

Figure 16 *The pressure distributions at third flow condition.*

Sensitivity to the fracture orientation

The fracture orientation has another significant effect on the flow response. While main large-scale fractures control the major flow distribution, the small-scale fractures distribution affects it as well. To estimate this influence, we generate a geological model shown in Figure 17 by removing most of the small-scale features in the geological model shown in Figure 9 when the angles are larger than 90 degrees. Using this model, we perform a similar sensitivity analysis as before. Again, the geometry parameters, relative permeability, fluid properties and injection/production strategy are taken from Tables 1-5 in Appendix A.

The saturation and pressure solutions are shown in Figures 18 and 19. The results demonstrate that MLDFM is capable to predict the flow response accurately compared with EDFM + ECM for different fracture orientations. The improvement in the accuracy of MLDFM compared with EDFM + ECM is equal to 80.1%.

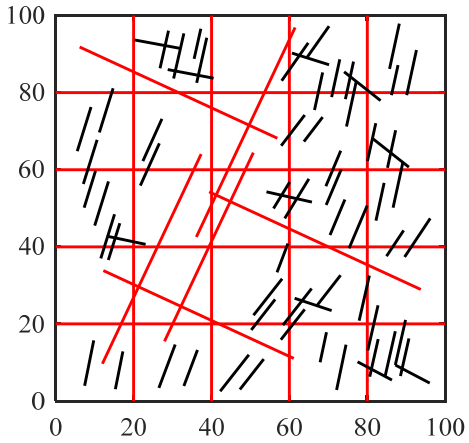

Figure 17 *The schematic of a fracture network.*

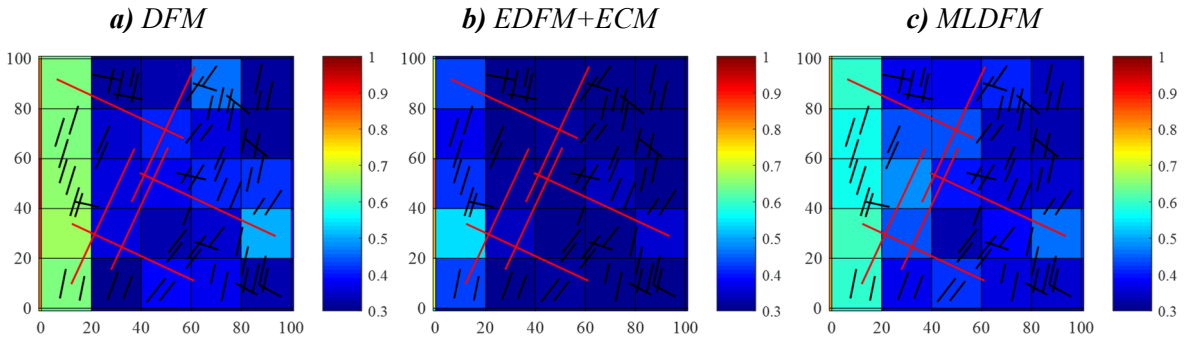

Figure 18 *The water saturation distributions at first flow condition.*

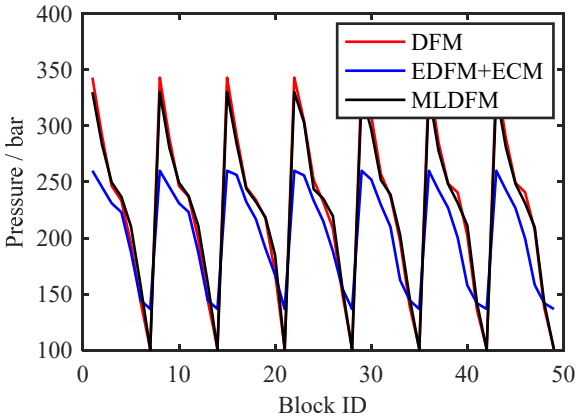

Figure 19 *The pressure distributions at first flow condition.*

Realistic fracture network

In this section, we will test MLDFM with a realistic complex fracture network shown in Figure 20. The fracture network is obtained from Apodi, Brazil. The reservoir dimension is 300×300 m, there is a water injection well at (75, 75) and a production well at (225, 225), the simulation time is 20,000 days, the other parameters needed are taken from Tables 1-5 in Appendix A.

The water saturation and pressure distributions obtained by DFM and MLDFM simulations are shown in Figures 21 and 22. It is clear that MLDFM can predict the main flow response accurately in realistic fracture networks. The number of control volumes corresponding to MLDFM and DFM are 1727 and 218456 respectively, and we can conclude that MLDFM is an accurate and computational efficient forward-simulation method for carbonate reservoirs.

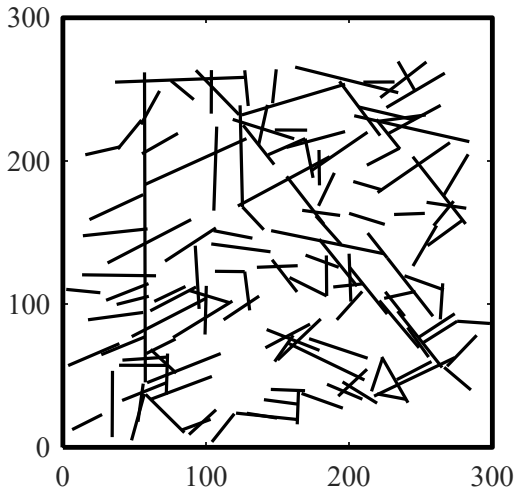

Figure 20 *A realistic fracture network.*

a) *The water saturation distribution obtained from DFM (volume weighted)*

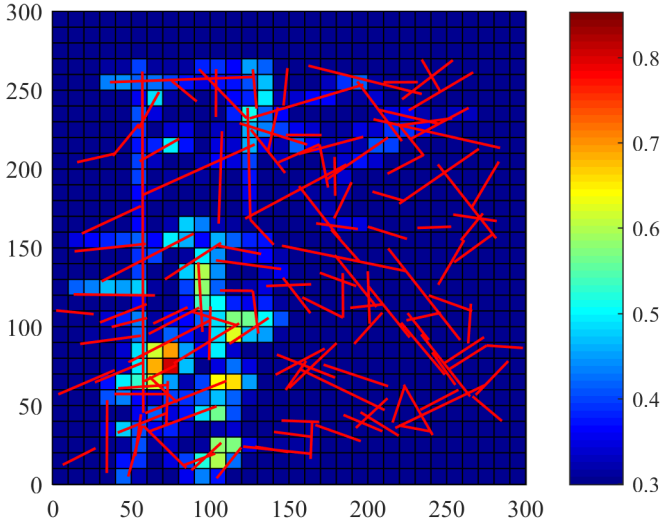

b) *The water saturation distribution obtained from MLDFM*

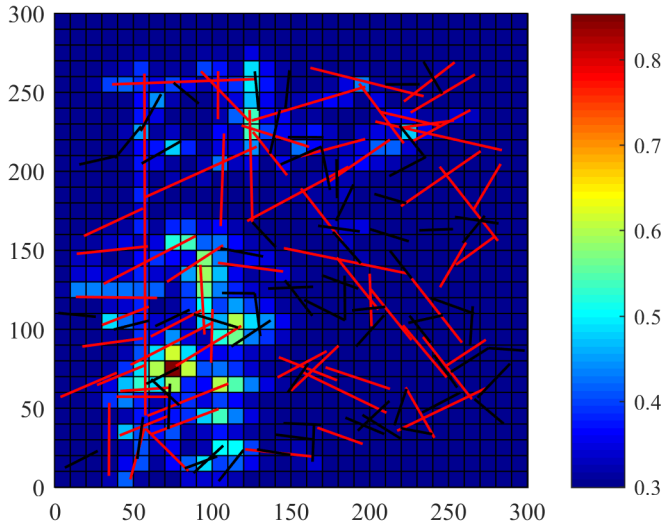

Figure 21 *The water saturation distributions obtained from MLDFM and DFM.*

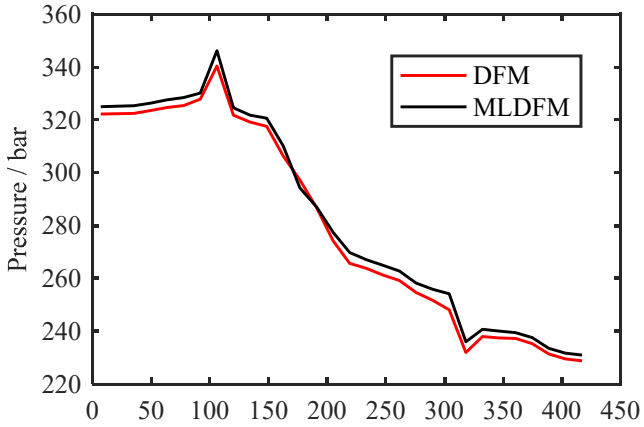

Figure 22 *The pressure solutions on the diagonal of geo-model.*

Conclusions

Due to the various multiscale features, the flow response in carbonate reservoir has a very complex structure. A multi-level discrete fracture model (MLDFM) has been proposed in this study to provide a robust and efficient forward-simulation approach for modelling of complex fractured reservoirs. In MLDFM, we represent a fractured reservoir as a triple continuum forward model where large fractures are treated explicitly using the numerical EDFM and small features are numerically upscaled as a third continuum. Therefore, the large-scale flow response is captured in the model by the application of Embedded DFM, and the small-scale flow response is captured by the third continuum. To make MLDFM feasible in practice, two levels of grids have been constructed and associated with each other. Among the two grid levels, the coarser one is based on a structured grid and used in global simulation. The finer level is based on unstructured DFM and used to resolve the flow response associated with small-scale features. As the multi-scale flow response depends on local boundary conditions, we apply the local-global upscaling formalism to update transmissibilities between different features once the local flow conditions have been changed. The test cases in this study demonstrate that MLDFM is capable to capture the multi-scale flow response in carbonate reservoirs accurately and efficiently, and is robust with respect to different flow conditions, fracture position, distributions and orientation.

Acknowledgement

We would like to thank the Stanford University Petroleum Research Institute for Reservoir Simulation (SUPRI-B) program for the permission to use ADGPRS in this work.

Nomenclature

k	Absolute permeability [μm^2]
k_r	Relative permeability of phases [-]
P	Reservoir pressure [10^{-1}MPa]
q	Sink/source per unit volume of reservoir [mol/cm^3/s]
S	Saturation of water, oil or gas phase [-]
t	Time [s]
V	Volume [cm^3]
$\mathbf{u}$	Darcy velocity of oil or gas phase [cm/s]
ϕ	Reservoir porosity [-]
ρ	Molar density of oil or gas phase [mol/cm^3]
μ	Viscosity [cP]
λ	Phase mobility [cP^{-1}]

Subscripts

m the matrix block
f the fracture element

Superscripts

n Time step level

References

Barenblatt G. I , Zheltov Iu. P , Kochina I. N., 1960. Basic concepts in the theory of seepage of homogeneous liquids in fissured rocks. Journal of Applied Mathematics and Mechanics 24(5), 1286-1303.

Chen, Y., Durlofsky, L. J., Gerritsen, M., Wen, X. H., 2003. A coupled local-global upscaling approach for simulating flow in highly heterogeneous formations. Advances in Water Resources 26(1): 1041-1060.

CMG, 2013. IMEX User Guide. Version 2013. Calgary, Canada.

Durlofsky, L. J., Chen, Y., 2012. Uncertainty quantification for subsurface flow problems using coarse-scale models. In I. G. Graham, T. Y. Hou, O. Lakkis, and R. Scheichl, editors, Numerical Analysis of Multiscale Problem, Lecture Notes in Computational Science and Engineering, 163-202.

Eclipse Technical Description, 2009. Schlumberger Simulation Software Manuals.

Gallyamov E., Garipov T., Voskov D., van den Hoek P., 2018. Discrete fracture model for simulating waterflooding processes under fracturing conditions, Int J Numer Anal Methods Geomech, doi:10.1002/nag.2797

Garipov, T. T., Tomin, P., Rin, R., Voskov D. V., Tchelepi H. A. 2018. Unified thermo-compositional-mechanical framework for reservoir simulation. Computational Geosciences. https://doi.org/10.1007/s10596-018-9737-5

Garipov, T.T., Karimi-Fard, M., Tchelepi, H.A., 2016. Discrete fracture model for coupled flow and geomechanics, Computational Geosciences, 20 (1), pp. 149-160. DOI: 10.1007/s10596-015-9554-z

Geuzaine, C., Remacle, J. F., 2009. Gmsh: a three-dimensional finite element mesh generator with built-in pre- and post-processing facilities. International Journal for Numerical Methods in Engineering 79(11), 1309-1331.

Gerke, H. H., van Genuchten, M. T., 1993a. A dual-porosity model for simulating the preferential movement of water and solutes in structured porous media. Water Resources Research 29: 305-319.

Gerke, H. H., van Genuchten, M. T., 1993b. Evaluation of a first-order water transfer term for variably saturated dual-porosity flow models. Water Resources Research 29: 1225-1238.

Gong, B., 2007. Effective models of fractured systems. Standford.

Hajibeygi, H., Karvounis, D., Jenny, P., 2011. A hierarchical fracture model for the iterative multiscale finite volume method. Journal of Computational Physics 230(24): 8729-8743.

Karimi-Fard, M., Durlofsky, L. J., 2016. A general gridding, discretization, and coarsening methodology for modeling flow in porous formations with discrete geo-logical features. Advances in Water Resources 96(6), 354-372.

Karimi-Fard, M., Durlofsky, L., 2012. Accurate resolution of near-well effects in upscaled models using flow-based unstructured local grid refinement. SPE Journal 1084-1095.

Karimi-Fard, M., Durlofsky, L. J., Aziz, K., 2004. An efficient discrete fracture model applicable for general-purpose reservoir simulators. SPE Journal 9(2), 227- 236.

Karimi-Fard, M., Gong. B., Durlofsky, L., 2006. Generation of coarse-scale continuum flow models from detailed fracture characterizations. Water Resources Research 42(10), W10423.

Lee, S. H., Jensen, C. L., Lough, M. F., 2000. Efficient finite-difference model for flow in a reservoir with multiple length-scale fractures. SPE Journal 5(3), 268-275.

Li, L., Lee, S. H., 2008. Efficient Field-Scale Simulation of Black Oil in a Naturally Fractured Reservoir Through Discrete Fracture Networks and Homogenized Media. SPE Journal 750-758.

Miller, C. T., Christakos, G., Imhoff, P. T., *et al*., 1998. Multiphase flow and transport modeling in heterogeneous porous media: challenges and approaches. Advances in Water Resources 21: 77-120.

Pruess, K., Narasimhan, T. N., 1982. On fluid reserves and the production of superheated steam from fractured, vapor-dominated geothermal reservoirs. Journal Geophysical Research 87(B11), 9329-9339.

Pruess, K., Narasimhan, T. N., 1985. A practical method for modeling fluid and heat flow in fractured porous media, SPE Journal 25(1), 14-26.

Renard, P., de Marsily, G., 1997. Calculating effective permeability: a review, Advances in Water Resources 20: 253-278.

Sartori, A., 2018. Uncertainty Quantification Based on Hierarchical Representation of Fractured Reservoirs. TU Delft.

Schlumberger Market Analysis, 2007.

Tene, M., Bosma, S. B., Al Kobaisi, M. S., Hajibeygi, H., 2017. Projection-based Embedded Discrete Fracture Model (pEDFM). Advances in Water Resources 105, 205-216.

Ţene, M., Wang, Y., Hajibeygi, H., 2015. Adaptive algebraic multiscale solver for compressible flow in heterogeneous porous media. Journal of Computational Physics 300: 679-694.

Voskov, D., 2012. An extended natural variable formulation for compositional simulation based on tie-line parameterization. Transport in porous media 92(3), 541-557.

Wang, Y., Hajibeygi, H., Tchelepi, H., 2014. Algebraic multiscale solver for flow in heterogeneous porous media. Journal of Computational Physics 259: 284-303.

Warren, J. E., Root, P. J., 1963. The behavior of naturally fractured reservoirs. SPE Journal 245-255.

Zaydullin, R., Voskov, D.V., James, S.C., Henley, H., Lucia, A., 2014. Fully compositional and thermal reservoir simulation, Computers and Chemical Engineering, 63, pp. 51-65. DOI: 10.1016/j.compchemeng.2013.12.008

Appendix A: Properties of simulation model

Table 1 *Geometry parameters.*

Parameter	Value	Unit
Reservoir dimensions	100×100	m
Reservoir thickness	10	m
Initial pressure	200	bar
Initial water saturation	0.3	
Matrix permeability	0.01	μm^2
Matrix porosity	0.2	
Fracture permeability	10000	μm^2
Fracture porosity	1.0	
Fracture aperture	0.001	m
Well radius	0.1	m

Table 2 *Relative permeability (Corey equation).*

Parameter	Value
Phase exponent	2
Oil exponent	4
Irreducible phase saturation	0
Residual oil saturation	0
End point of the oil relative permeability curve	1

Table 3 *Oil formation volume and viscosity.*

Pressure	Formation volume (rm^3/sm^3)	Viscosity (cP)
50.0	1.97527	0.21564
70.0	1.96301	0.21934
90.0	1.95464	0.21981
110.0	1.93391	0.22325
130.0	1.91309	0.22736
150.0	1.89217	0.2317
170.0	1.87115	0.23628
190.0	1.85005	0.24112
210.0	1.82887	0.24623
230.0	1.80761	0.25165
250.8	1.78628	0.25738

Table 4 *Fluid densities (surface condition).*

Oil density (Kg/m^3)	Water density (Kg/m^3)
800	1000

Table 5 *Injection/Production strategy.*

Parameter	Value	Unit
Injection rate	500	m^3/d
Production rate	500	m^3/d
Simulation time	10000	d